

Optical imaging techniques for the study of malaria

Sangyeon Cho¹, Soomin Kim², Youngchan Kim² and YongKeun Park^{2,3}

¹ Department of Chemistry, Korea Advanced Institute of Science and Technology, Daejeon, 305-701, Republic of Korea

² Department of Physics, Korea Advanced Institute of Science and Technology, Daejeon, 305-701, Republic of Korea

³ Institute for Optical Science and Technology, Korea Advanced Institute of Science and Technology, Daejeon, 305-701, Republic of Korea

Malarial infection needs to be imaged to reveal the mechanisms behind malaria pathophysiology and to provide insights to aid in the diagnosis of the disease. Recent advances in optical imaging methods are now being transferred from physics laboratories to the biological field, revolutionizing how we study malaria. To provide insight into how these imaging techniques can improve the study and treatment of malaria, we summarize recent progress on optical imaging techniques, ranging from *in vitro* visualization of the disease progression of malaria infected red blood cells (iRBCs) to *in vivo* imaging of malaria parasites in the liver.

Light microscopy to study malaria

Malaria is a mosquito-borne infectious disease caused by a protozoan parasite. Malaria-inducing parasites, transmitted by mosquitoes, invade host liver cells and red blood cells (RBCs). The parasites cause structural and biochemical modifications in cells during invasion, growth and egress. Every year, malaria infects approximately 250 million people, especially young children in sub-Saharan Africa [1,2] (see Box 1 for detailed malaria facts). The malaria infection cycle begins when malaria-inducing parasites, transmitted by infected mosquitoes, infect liver cells, resulting in multiplied merozoites (see Glossary and Box 2). These merozoites then enter the bloodstream and invade host RBCs, where they undergo 48 h of intraerythrocytic development before causing the cell membrane to erupt. Upon invasion, the malaria parasite causes structural, biochemical and mechanical alterations to host RBCs. Subsequent molecular and cellular events are tightly regulated by the biochemical pathways of the parasite, therefore they influence the severity of the disease. The mechanisms by which malaria-inducing parasites invade, grow and exit host RBCs are complex and not fully understood.

Light microscopy techniques have unique advantages for malaria studies and have contributed to some significant advances in the understanding of the disease. The non-invasive nature of light allows for imaging of live cells under physiological conditions. Fluorescent protein labels further allow specific proteins to be imaged in living cells. However, optical properties such as refractive index and fluorescence lifetime can be used to retrieve useful biochemical information about malaria pathophysiology.

Although non-optical imaging techniques including soft X-ray microscopy [3] and atomic force microscopy [4] can provide extremely high spatial resolving power, these techniques are limited to quasi-static or *ex vivo* imaging. In this review, we summarize recent light microscopy techniques used to study malaria.

In vitro optical imaging of infected red blood cells (iRBC) using exogenous labeling agents

DNA/RNA staining methods

Malarial detection methods in cytogenetics and for histopathological diagnosis have relied on DNA staining, where Giemsa stain is used to label parasite DNA in blood smears. Although Giemsa staining was first developed more than 100 years ago, it is still the most common technique in the imaging and diagnosis of malaria (Figure 1a). A thin smear can be used to identify malaria

Glossary

Birefringence: having two refractive indices, depending on the polarization of light. When light passes through a birefringent material, it may split into two due to the double refractions.

Food vacuole: vacuole in which ingested food is digested.

Förster resonance energy transfer (FRET): a distance-dependent optical mechanism that transfers energy from a donor to an acceptor. Energy transfer efficiency is proportional to the inverse of the sixth power of the distance.

Gametocyte: malaria parasite in the sexual stage. Gametocytes produce gametes when taken into the mosquito.

Hemozoin: insoluble crystallized form of hemes. Blood feeding parasites such as *P. falciparum* degrade hemoglobin (Hb). Because of the toxicity of free heme, the parasite crystallizes hemes as an insoluble biocrystal.

Interferogram: intensity pattern produced by interference of multiple waves. An interferogram can be used to record the optical phase delay.

Intraerythrocytic stage: stage when the parasite invades and locates inside the red blood cell.

Merozoite: any of various cells produced by multiple fission in the asexual stage of the parasite life cycle.

Parasitemia: quantitative contents of parasites present in the blood.

Parasitophorous vacuole: vacuole in which the parasite resides during the intraerythrocytic stage.

Raman scattering: inelastic light scattering. Scattered light has a different frequency than incident light. Because a Raman frequency shift occurs with a change in a molecule's energy status, Raman scattering can be used to identify molecular features.

Refractive index: an intrinsic optical property of a material, defined as the ratio of the speed of light in vacuum to the speed in a given material.

Sporozoite: spore formed after fertilization.

Third harmonic generation (THG): a material-dependent nonlinear optical effect where three photons interact with a nonlinear material to effectively form a new photon with triple the energy.

Two-photon absorption fluorescence (2PAF): a fluorescence process wherein a molecule is excited by simultaneously absorbing two photons of identical or different frequencies. The excitation energy is equal to the sum of the energies of the two photons.

Box 1. Malaria facts**Etiology of malaria**

Cases of malaria are spread throughout Asia and sub-Saharan Africa [70]. Every year, there are about 250 million cases of malaria infection and more than 700,000 deaths [71]. Malaria is caused by the intracellular protozoan parasites of the genus *Plasmodium*, which is transmitted by the *Anopheles* mosquito. Symptoms of malaria include fever, headache, vomiting, arthralgia and anemia. Clinical deterioration exhibits between 3 and 7 days after the onset of major symptoms [72].

Species of malaria parasite

Four species of *Plasmodium* infect humans and cause malaria: *Plasmodium falciparum* (*P. falciparum*), *P. vivax*, *P. malariae* and *P. oval*. The two main causes of malaria disease are *P. falciparum* and *P. vivax*. Not all species of parasites are fatal: *P. falciparum* is the most fatal parasite and causes the most deaths. *P. vivax* is not as lethal as *P. falciparum*, but it still results in serious disability for infected people [73].

Changes in iRBCs

The intraerythrocytic cycle leads to structural, biochemical and mechanical alterations to host RBCs. The structural changes of iRBCs include the development of parasitophorous vacuoles, which enclose the growing parasites, and the formation of adherent protrusions or 'knobs' on the RBC membrane. Major biochemical alterations include the digestion of cytosolic Hb proteins, which are then converted into hemozoin, polymerized forms of heme. Mechanical modifications include a loss of RBC deformability and an increase of adherence of iRBCs to the vascular endothelium or other RBCs. During the intraerythrocytic cycle, parasites express proteins (including RESA, KAHRP, PfEMP and MESA, etc.), which are known to interact with host iRBCs and make iRBCs less deformable. Furthermore, the rigidity and viscosity of the intracellular parasite itself also increases cell rigidity. RBCs infected with *P. falciparum* bind to vascular endothelium and they can avoid being eliminated by the spleen. The *P. falciparum* infected RBC becomes spherical, which has a lower deformability [74].

species and quantify parasitemia. Thick smears are 20–40 times more sensitive than thin smears. The advantages of DNA staining with Giemsa stain are low cost and the possibility of identifying the species of *Plasmodium* parasites

[5]. Giemsa staining is, however, a time-consuming process and difficult to synchronize with other methods such as antigen detection. The quality of the diagnosis also depends on the skill and experience of the microscopist.

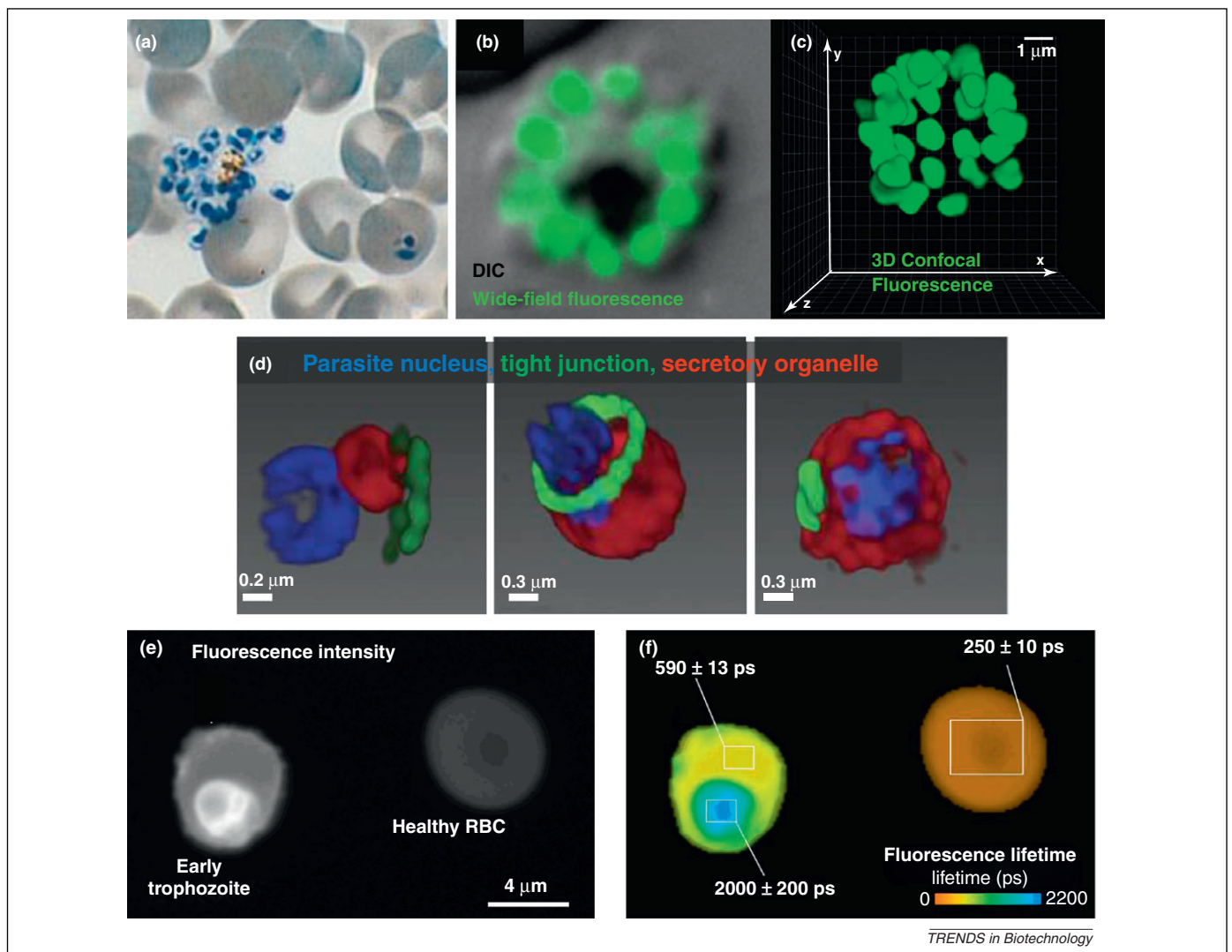
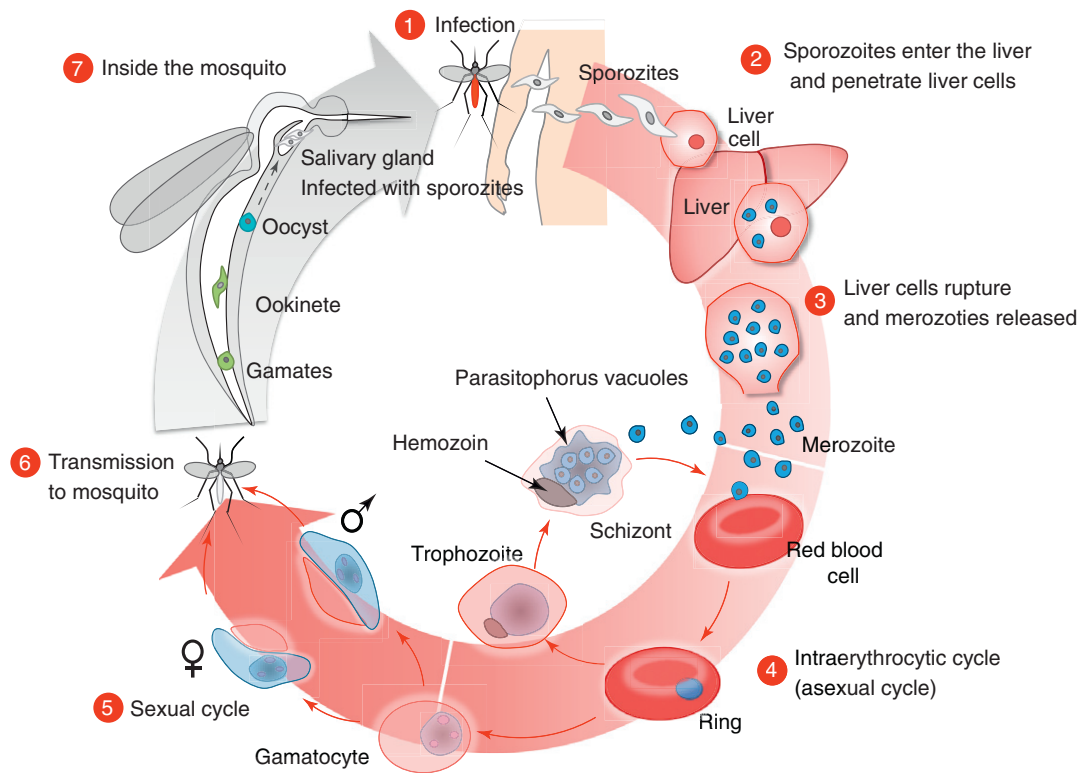


Figure 1. *In vitro* optical imaging techniques using exogenous labeling agents. (a) Bright field microscopic images of Giemsa-stained *Plasmodium vivax* infected red blood cells (iRBCs) including mature schizonts releasing merozoites (left) and a ring stage (right). Reproduced, with permission, from [66]. (b) Differential interference contrast (DIC) image (gray) of schizont stage iRBC merged with wide-field fluorescence image from merozoites (green). (c) 3D reconstructed images of merozoites from the iRBC in (b). Reproduced, with permission, from [67]. (d) Time-lapse image of the malaria parasite invasion acquired by 3D structured illumination microscopy (SIM). Reproduced, with permission, from [20]. (e,f) Fluorescence intensity image of an early trophozoite iRBC and a healthy RBC (e), and its fluorescence lifetime image (f). Reproduced, with permission, from [68].

Box 2. The life cycle of the malaria parasite

- (1) The malaria infection cycle starts when infected female mosquitoes of the *Anopheles* genus feed on people (Figure 1). When mosquitoes ingest human blood, malaria parasites in the form of sporozoites are injected into human subcutaneous tissue (less frequently the bloodstream) [75].
- (2) Then, the sporozoites travel to the bloodstream and invade liver cells (hepatocytes). Inside the hepatocytes, each sporozoite rapidly grows into tens of thousands of merozoites, over a time period of about 6 days [73].
- (3) When the hepatocytes rupture, the parasites in the form of merozoites are released and enter the blood stream. Then, the merozoites can invade RBCs and initiate the intraerythrocytic cycle.
- (4) During the intraerythrocytic cycle (ring to trophozoite to schizont stage) of approximately 48 h, merozoites grow and multiply inside the RBCs, causing dramatic alterations in the structural and biochemical properties of the host RBCs (Box 1). Once the merozoite invades the RBCs, these merozoites become un-nucleate and are said to be in the ring stage. This is followed by the stage of trophozoites, which develop into multi-nuclei cells called schizonts. Then schizonts divide and create many merozoites again. When newborn merozoites are well ripened, the RBCs rupture and the resulting egressed merozoites cause secondary infections in other RBCs. During this rupture, toxic materials also spread into the human body to cause numerous malaria symptoms including fever and shivering.
- (5) Not all merozoites reproduce themselves identically during the intraerythrocytic cycle; some merozoites turn into gametocytes, capable of producing male and female gametes, which do not rupture.
- (6) Interestingly, these gametocytes cannot create male and female gametes in the human host, and they need to be extracted by the mosquito again.
- (7) When the gametocytes re-enter the mosquito's body, they turn into male and female gametes. They fuse together and develop in the mosquito's intestines, and finally differentiate into oocysts. In these oocysts, a numbers of mitotic divisions occur and the parasites again become sporozoites. Newborn sporozoites move to the mosquito salivary gland and, if the insect again feeds on a human, the malaria cycle starts all over again. All human malaria-inducing parasites invade by the same mechanism; *P. falciparum* infects RBCs more effectively as a result of its highly flexible receptor pathways, which are related to the invasion process [74].



TRENDS in Biotechnology

Figure 1. The life cycle of the malaria parasite.

An alternative to imaging blood smears with Giemsa is to stain parasite RNA with acridine orange (AO). Intraerythrocytic malarial parasites are rich in RNA, which emits red fluorescence after AO staining [6]. Both thin and thick smears are easier to read with AO stain than with Giemsa stain because artifacts or pigment dots, which are troublesome in the Giemsa stain, do not occur [7]. In addition, AO provides rapid results: diagnostic results are readily obtained within 5 min, whereas with Giemsa staining this process may take 45 min or even longer [6].

Wide-field and confocal fluorescence microscopy

Fluorescence microscopy has been extensively used to (i) study live iRBCs [8], (ii) detect the malaria parasite [9], and (iii) quantify the volume and membrane area of iRBCs [10]. Wide-field fluorescence microscopy rapidly provides 2D fluorescence images (Figure 1b). Confocal fluorescence microscopy employs the principles of point illumination and point detection to provide 3D fluorescence images (Figure 1c). In confocal microscopy, the addition of a pinhole enables optical sectioning by suppressing the

out-of-focus light. Also, the use of a pinhole can enhance both lateral and axial resolution but with the cost of signal loss. Depending on the method of scanning excitation focused beams, confocal fluorescence microscopy can be classified into confocal laser scanning microscopy or spinning disk confocal microscopy [11].

Different fluorophores have been used to study malaria, depending on their target molecules and applications. Giemsa and AO (to label parasite DNA and RNA) can be imaged by wide-field and confocal fluorescence microscopy. Fluorescent proteins have been employed for selective imaging of a target malaria protein. To establish and maintain infection during the intraerythrocytic cycle, a malaria parasite secretes proteins, such as knob-associated histidine-rich protein (KAHRP), ring-infected erythrocyte surface antigen (RESA), glycophorin binding protein-130 (GBP-130), Rho in filopodia (RiF) and *Plasmodium falciparum* erythrocyte membrane protein 1 (PfEMP1), to the host RBC, which can be labeled with fluorescence proteins and imaged with wide-field fluorescence microscopy. Fluorescence proteins have been used to study protein translocation through the parasitophorous vacuole membrane and into the erythrocyte [12]. Organic fluorophores can also be used for functional imaging. A pH-sensitive dye (pHluorin) was used to quantify the acidity level in the parasites [13]. A calcium sensitive dye (Fura Red) was employed to image and determine the accumulation of Ca^{2+} in the parasite food vacuole [14].

Quantum dots (QDs), nanometer-sized semiconductor crystals, have shown potential as a new immunochemical probe to study living cells. QDs are remarkably photostable, resist photobleaching and have high quantum yields [15]. QDs were used to study RBC membrane modifications during the invasion of parasites [16,17]. Recently, immunofluorescence assays with QDs showed their potential to detect parasite growth and for anti-malaria drug assays [17].

Super resolution nanoscopy

The optical resolving power of conventional imaging systems is limited by diffraction, so that objects separated closer than half of the wavelength of light (approximately 200–300 nm) cannot be resolved. Considerable effort has pushed the spatial resolution of optical imaging to the nanometer scale. Recently, several imaging techniques have demonstrated super resolution optical imaging: stimulated emission depletion (STED), photo-activated localization microscopy (PALM), stochastic optical reconstruction microscopy (STORM), structured illumination microscopy (SIM) and other super resolution nanoscopy techniques can provide optical images with a resolution of a few tens of nanometers [18].

Recently, SIM became the first super resolution optical nanoscopy to contribute significantly to malaria research. By illuminating samples with multiple structured light patterns and reconstructing the images, SIM allows precise visualization of target samples that are below the diffraction limit [19]. Using SIM, the critical moment of the parasite invasion into RBCs was visualized with unprecedented resolution [20] (Figure 1d). This study demonstrated the relevance of super resolution nanoscopy in malaria research, especially the localization of malaria-related

proteins at a lateral resolution of ~ 118 nm and a vertical resolution of ~ 280 nm.

In current super resolution nanoscopy techniques, high spatial resolution is obtained while sacrificing the temporal resolution, and thus super resolution nanoscopy is generally slower than conventional fluorescent microscopy. The achievement of high temporal resolution in super resolution nanoscopy is an active research topic [21]. Super resolution nanoscopy techniques, with a better temporal resolution, may play a critical role in revealing the mechanisms of malaria infection by providing detailed spatio-temporal localizations and interactions of malaria-related proteins.

Förster resonance energy transfer (FRET) and fluorescence lifetime imaging microscopy (FLIM)

FRET refers to the non-radioactive energy transfer from an optically excited donor molecule close to an acceptor molecule (typically less than 10 nm). Because the FRET signal is highly sensitive to the distance between the donor and the acceptor, it is used for quantitative imaging of the presence or interactions between molecules. In malaria research, especially for functional iRBC imaging, FRET has been employed to detect mutation-related genotyping resistance to observe the targeting of ligands or inhibitors to the parasite, and to rapidly differentiate between different *Plasmodium* species [22].

FLIM is based on the time it takes the fluorescence signal to decay (lifetime), rather than its intensity. The fluorescence lifetime of a fluorophore can be affected by both radiative fluorescence and non-radiative FRET processes. Energy transfer from a donor to an acceptor molecule decreases the lifetime of the donor. Thus, FRET measurements using FLIM provide a useful method for probing the environments of the fluorophore [23]. This method was used to measure the hemoglobin (Hb) concentration in the cytosol of live iRBCs (Figure 1e,f) [24]. Hb is an effective quencher of any fluorophore emitting fluorescence below 600 nm, and the emission spectrum of calcein overlaps with the absorption spectrum of Hb. Because FRET will occur from calcein to neighboring Hb in close proximity, the absorption of Hb was measured and then used to estimate Hb concentration in the iRBC cytosol [24].

In vitro optical imaging of iRBC with intrinsic optical signals

Polarization microscopy

Polarization microscopy effectively images birefringent material and has been used in malaria research since the 1980s [25]. Merozoites and hemozoin in mature stage parasites have a distinct birefringence [26]. Cross- or orthogonal polarization imaging can enhance an image contrast for these merozoites and hemozoin. Polarization microscopy is almost twice as sensitive as conventional light microscopy without the use of polarization when it comes to detecting hemozoin and *Plasmodium* [26]. Polarized light has also been successfully used to diagnose malaria in a flow cytometer [27].

Differential interference contrast (DIC) microscopy

DIC microscopy was devised in the 1950s as an optical microscopy technique for rendering contrast in unstained

transparent specimens [28]. In DIC microscopy, an optical phase shift, which depends on the refractive index and the thickness of a specimen, is transformed to a measurable light intensity contrast by using the principle of interferometry: two beams are separated by a Wollaston prism depending on their polarization [29]. Without any exogenous labeling agents, DIC microscopic images can reveal the morphologies and subcellular structures of iRBC (Figure 2a). However, because DIC image contrast is based on an optical phase shift, the method does not provide molecular-specific information. Nevertheless, DIC microscopy has been used to directly quantify malaria parasite release in iRBCs [30] and to investigate how malaria parasites egress from mature schizonts [31].

Dark-field microscopy

Dark-field microscopy uses a simple illumination technique, but still dramatically enhances contrast in unstained samples. The principle of dark-field microscopy is to illuminate a sample with light but only image the light scattered from the sample. Dark-field microscopy has been used to image the iRBC since the 1930s [32,33]. Dark-field microscopy provides high contrast images of hemozoin [33] because hemozoin generates a strong light scattering signal (Figure 2b). Recently, dark-field illumination integrated with polarization microscopy was reported to enhance the scattering contrast for hemozoin in a blood smear [34].

Dark-field microscopy effectively detects light scattering from hemozoin without using exogenous labeling. However, the technical limitation of dark-field microscopy is specificity; it may be difficult to distinguish between the desired light scattering signal and those of other small scattering particles in the sample. Yet dark-field illumination can serve as a powerful means to diagnose malaria by

effectively collecting the light signal from hemozoin for other measurements (e.g. spectroscopic measurement, as presented in [34]).

Quantitative phase imaging (QPI)

Quantifying the optical phase shifts across biological cells and tissues provides information about morphology and dynamics. QPI is an effective optical imaging technique to study the pathophysiology of RBCs because QPI measures the morphology and dynamic membrane fluctuations of RBCs at a nanometer scale [35]. QPI employs the principle of laser interferometry to quantitatively retrieve the optical field information of the cells, especially the optical phase delay [36]. QPI does not require any exogenous agents for imaging because Hb proteins provide the optical phase shift. Because the RBC cytoplasm consists primarily of Hb protein solution, the topological information of RBC can be directly retrieved from the measured optical phase delay. Topographical images of the intraerythrocytic cycle of *P. falciparum* iRBCs have been shown using diffraction phase microscopy (DPM) [37,38], a highly stable common-path microscopy for QPI (Figure 2c).

QPI is capable of imaging live cell dynamics at the millisecond time scale. Thus, QPI can also provide the biomechanical properties of RBC membranes by measuring and analyzing their dynamic membrane fluctuations. Dynamic cell membrane fluctuations correlate strongly with the structures of the cell membrane cortex and can be altered by biochemical changes [39,40]. Measuring the membrane fluctuation dynamics of iRBCs allows for the non-invasive retrieval of the mechanical property (shear modulus) through the use of an appropriate mechanical model [41].

In addition, optical field information measured by QPI can be combined with Fourier transform light scattering

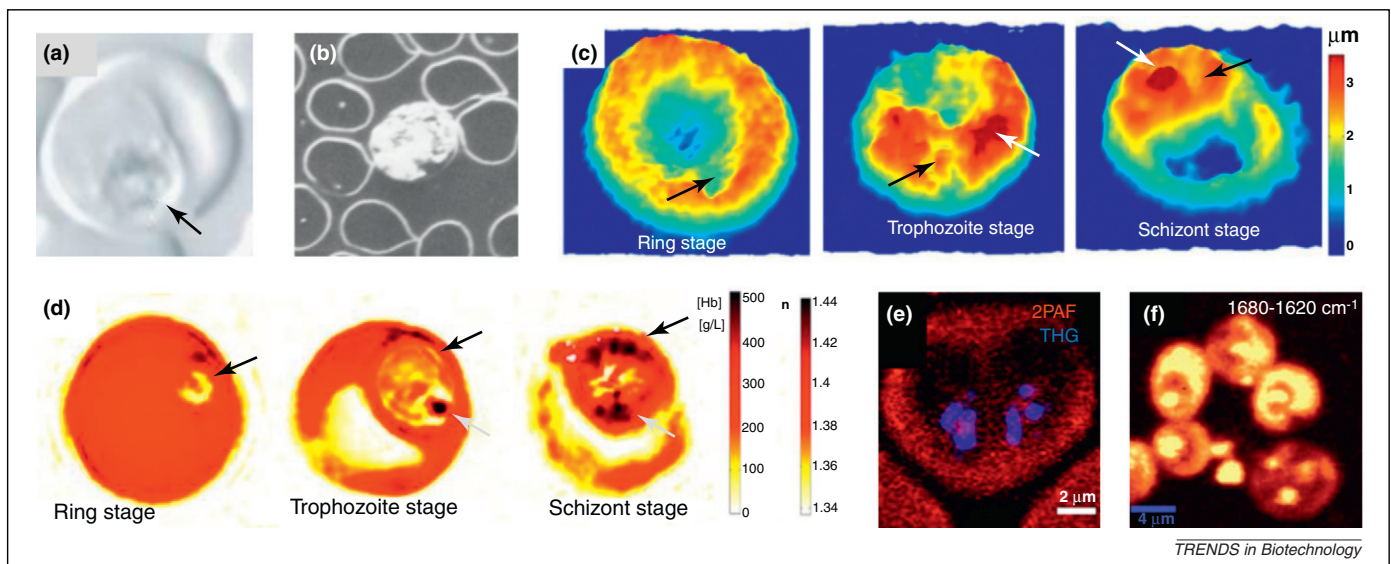


Figure 2. *In vitro* optical imaging techniques of infected red blood cell (iRBC) based on intrinsic optical signals. (a) Differential interference contrast (DIC) image of trophozoite stage of iRBC. The arrow indicates the malaria parasite food vacuole. Reprinted, with permission, from [69]. (b) Microscopic image of schizonts of *Plasmodium vivax* acquired from dark-field microscopy [33]. (c) Topographic images of a healthy RBC and iRBCs at different intraerythrocytic stages measured by quantitative phase microscopy. The black and white arrows indicate the location of parasitophorous vacuoles and hemozoin, respectively. Reprinted, with permission, from [41]. (d) Cross-sectional images of 3D refractive index tomograms of a healthy RBC and iRBCs at different intraerythrocytic stages measured by tomographic phase microscopy. The black and white arrows indicate the location of parasitophorous vacuoles and hemozoin, respectively. Reprinted, with permission, from [49]. (e) Two-photon absorption fluorescence (2PAF, red) and third harmonic generation (THG) microscopic image of iRBC. Reprinted, with permission, from [49]. (f) Resonance Raman (RR) image of iRBCs. Chemical map is generated by integrating over the Raman shift between 1680 and 1620 cm^{-1} . Reprinted, with permission, from [51].

(FTLS) analysis to provide light scattering spectroscopic information [42]. The light scattering spectroscopy pattern is identical to the intensity map of the optical field propagated to the far-field, which can be numerically calculated by Fourier transform of the optical field. Light scattering spectroscopy of RBCs can be used to measure the size of the RBC and Hb concentration [43] and to study membrane properties [44]. Recently, QPI and FTLS have been employed to provide the static and dynamic light scattering patterns of iRBCs [45]. The study demonstrated that light scattering signals of iRBCs can be used to distinguish iRBCs from uninfected RBCs.

Refractive index tomography

3D distribution of the refractive index can provide information about the structure and biochemistry of biological samples. The 3D refractive index tomogram of *P. falciparum* iRBCs was measured at various intraerythrocytic stages [41]. In another study, the 3D refractive index tomogram was measured with tomographic phase microscopy (TPM) [46]. TPM records multiple 2D field images in an interferometric microscope by sweeping the illumination beam. The multiple 2D projection optical field images are then used to reconstruct a 3D tomogram with an inverse Radon transform.

The 3D refractive index distribution of iRBCs can be used to visualize the complex structures of iRBCs including host RBC membrane shape, parasitophorous vacuoles and hemozoin [41] (Figure 2d). In addition, because the refractive index of the cytosolic Hb solution is linearly proportional to its concentration, Hb concentrations in iRBCs have been retrieved from 3D refractive index tomograms. Recently, 3D refractive index tomograms were measured for the last schizonts stages of the iRBC to study the parasite's egress mechanism [47].

Refractive index tomography offers a potentially useful means for linking refractive index with the pathological condition of the iRBC. Refractive index is an intrinsic optical signal that is directly related to the Hb concentration, an important pathological property of the iRBC. However, the current method used to measure the 3D refractive index has some technical limitations: the spatial resolution is still limited by optical diffraction; the tomographic reconstruction process requires a heavy computation and the inverse Radon transform does not consider diffraction of light, which may lead to inaccurate refractive indices.

Third harmonic generation (THG) and two-photon absorption fluorescence (2PAF) imaging

THG is a nonlinear optical effect. In THG, three photons interact with a nonlinear material effectively to form a new photon with tripled energy. The THG optical frequency triples and the wavelength shortens threefold compared with the incident photon. Unlike fluorescence emission, THG is a coherent process based on photon scattering. Thus, THG emission is highly directional and polarized where optical phase information is maintained. THG has been extensively used in bioimaging, especially to visualize nonlinear optical biomaterials including collagen, microtubules and muscle myosin [48].

THG imaging has proven to be a promising technique to efficiently image hemozoin [49]. THG has been used to detect hemozoin in live iRBCs. The THG signal from hemozoin can be explained by the molecular structure and composition of hemozoin (Figure 2e). THG imaging has several advantages for malaria research: no need for exogenous labeling, high signal to noise ratio, and high specificity for hemozoin, which may be useful for sensitive and rapid hemozoin screening. In addition, THG imaging can readily combine with 2PAF imaging because THG requires a pulsed laser, which can be shared with 2PAF microscopy. There is an intrinsic 2PAF signal from Hb proteins, which can be superimposed with THG images to visualize iRBCs (Figure 2e). However, this pulsed laser source is expensive, limiting many researchers from the full advantage of THG imaging.

Resonance Raman (RR) microscopy

RR microscopy is a promising way to diagnose iRBCs. RR microscopy is a variant of normal Raman scattering spectroscopy. In RR microscopy, the excitation beam overlaps with an electronic transition of particular target molecules, which enhances the resonance and thus sensitivity in Raman scattering imaging as a result of the combined effect of the absorption band. The intensity of each Raman signal depends on the wavelength of the excited beam and the vibrational modes of target molecules [50].

RR microscopy requires no additional staining, and there is no need for fluorophores to be applied to living cells. Light absorptive biomolecules such as hemozoin (malaria pigment), which is spectroscopically identical to its synthetic analogue β -hematin, have intense Raman signals with good signal to noise ratio. RR microscopy combined with conventional light microscopy has been used to investigate the localization of hemozoin in *in situ* conditions (Figure 2f) [51]. When combined with optical tweezers [52], an individual iRBC can be optically trapped and the physiological conditions of the iRBC can be studied by RR.

In vivo optical imaging of malaria infection

Recent advances in transgenic fluorescent and bioluminescent *Plasmodium* parasites have extended the possibility for real-time *in vivo* studies of the parasite's infection mechanisms [53]. Real-time *in vivo* optical imaging of iRBC or the interactions of malaria parasites within hepatocytes will provide exciting insights about the disease mechanism of malaria parasites, and can be used to evaluate strategies to effectively treat and prevent malaria.

Real-time *in vivo* imaging of iRBCs infected with a transgenic parasite that expresses luciferase has provided sequestration patterns that can be quantitatively analyzed (Figure 3a) [54]. To study the liver stage development of malaria in humans and rodents, modified luciferase-containing malaria parasites (*PbGFP-Luc_{con}*) were used in both cultured hepatocytes and the liver of living mice (Figure 3a) [55]. The quantitative analysis of liver stage development by real-time luminescence imaging is simpler and faster than with the RT-PCR method, therefore luminescence imaging is expected to assist the evaluation of

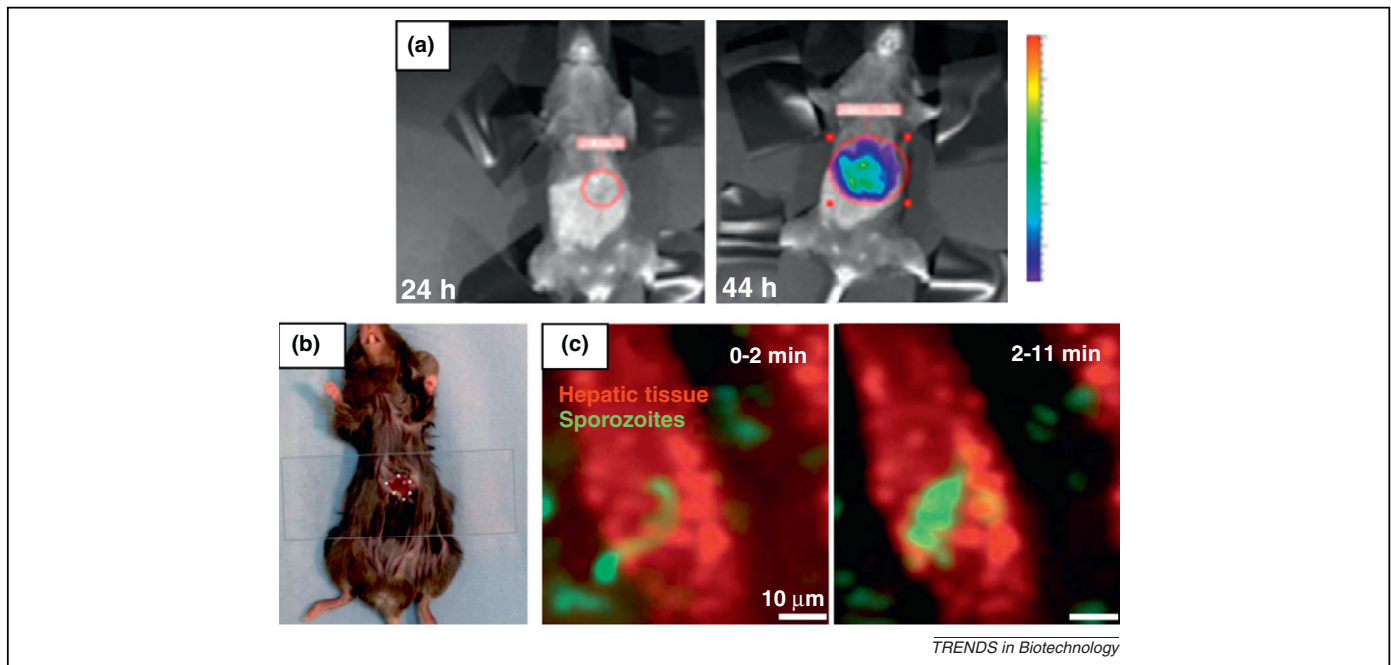


Figure 3. *In vivo* imaging of malaria infection. (a) Luminescence images of luciferase-expressing schizonts overlaid with a photographic image in a live mouse. Color bar indicates the relative levels of luciferase activity. Reprinted, with permission, from [55]. (b) C57BL/6 mouse prepared for *in vivo* fluorescence imaging of the liver. (c) *In vivo* fluorescence imaging of green fluorescent protein (GFP)-expressing sporozoites in the hepatic tissue of the mouse in (b). A sporozoite glides from the parenchyma into the sinusoid and back again into the parenchyma. Reprinted, with permission, from [56].

drug and vaccine effectiveness on *P. falciparum* infection without surgery or other invasive processes.

In vivo imaging studies of the liver stage of *Plasmodium* parasites have shown promise in elucidating the pathology of how parasites interact with host hepatocytes (Figure 3b,c) [56]. Laser scanning confocal fluorescence microscopy has been used to visualize the moment when sporozoites cross the liver sinusoid endothelial barrier from the sinusoidal lumen [57]. Moreover, spinning disk confocal microscopy has captured the moment that hepatic merozoites enter the blood circulation from infected hepatocytes [58].

Concluding remarks

The research work reviewed here suggest that various optical imaging methodologies may play an important role in enhancing the understanding of the pathophysiology of malaria, which can make a critical impact on the future assessment and treatment of the disease.

The uses of optical imaging techniques for studying malaria have not yet been fully explored; there are still many important issues in the study of malaria that can be tackled by the clever development and use of novel optical imaging techniques. New techniques are particularly needed to reveal the details of the underlying genetic and molecular mechanisms behind the parasite–host interaction. For example, the egress mechanism of merozoites from iRBCs and the role of the related proteins can be revealed by high-speed super resolution nanoscopy combined with an appropriate genetic knockout approach, e.g. SIM captured the invasion of merozoites into RBCs [20].

Furthermore, this emerging field of research can also assist in the development of effective diagnostic strategies that can be used in the harsh field environment. For example, the on-chip optical technique [59,60] can miniaturize optical components. These tools potentially enable

point-of-care diagnosis and treatment of the malaria in a portable and disposable platform that does not require a skilled microscopist.

In addition, light manipulation techniques can be integrated with optical imaging to revolutionize the way in which biologists approach questions in the study of malaria. The optical trapping technique has been used to measure the stiffness of iRBCs as the disease progresses [61,62]. Optical tweezers can be used to isolate individual living cells [63] for a very well controlled single cell imaging. For example, specific target iRBCs or parasites can be isolated in a blood smear, imaged and manipulated optically.

Recent developments in biotechnology have been effectively transferred from bench top to bedside due to close interdisciplinary collaborations [64,65]. To successfully address important issues in malaria research with new approaches in optical imaging techniques, it is crucial to develop interdisciplinary collaborations among clinicians, biologists, engineers and physicists. Considering the recent exponential growth of the field, we are optimistic that optical imaging techniques will play important roles in the study, diagnosis and assessment of malaria.

Acknowledgments

The support provided by KAIST (N10110038, N10110048, N01110446 and G04100075) is gratefully acknowledged.

References

- Enayati, A. and Hemingway, J. (2010) Malaria management: past, present, and future. *Annu. Rev. Entomol.* 55, 569–591
- Greenwood, B. and Mutabingwa, T. (2002) Malaria in 2002. *Nature* 415, 670–672
- Magowan, C. *et al.* (1997) Intracellular structures of normal and aberrant *Plasmodium falciparum* malaria parasites imaged by soft X-ray microscopy. *Proc. Natl. Acad. Sci. U.S.A.* 94, 6222

- 4 Nagao, E. *et al.* (2000) *Plasmodium falciparum*-infected erythrocytes: qualitative and quantitative analyses of parasite-induced knobs by atomic force microscopy. *J. Struct. Biol.* 130, 34–44
- 5 Jonathan, M. (2008) Sensitive detection of malaria infection by third harmonic generation imaging. *Biophys. J.* 94, L26
- 6 Keiser, J. *et al.* (2002) Acridine Orange for malaria diagnosis: its diagnostic performance, its promotion and implementation in Tanzania, and the implications for malaria control. *Ann. Trop. Med. Parasitol.* 96, 643–654
- 7 Kawamoto, F. (1991) Rapid diagnosis of malaria by fluorescence microscopy with light microscope and interference filter. *Lancet* 337, 200–202
- 8 Shute, G. and Sodeman, T. (1973) Identification of malaria parasites by fluorescence microscopy and acridine orange staining. *Bull. World Health Organ.* 48, 591
- 9 Kawamoto, F. and Billingsley, P. (1992) Rapid diagnosis of malaria by fluorescence microscopy. *Parasitol. Today* 8, 69–71
- 10 Esposito, A. *et al.* (2010) Quantitative imaging of human red blood cells infected with *Plasmodium falciparum*. *Biophys. J.* 99, 953–960
- 11 Pawley, J.B. (ed.) (2006) *Handbook of Biological Confocal Microscopy*, Springer Verlag
- 12 Marti, M. *et al.* (2004) Targeting malaria virulence and remodeling proteins to the host erythrocyte. *Science* 306, 1930
- 13 Kuhn, Y. *et al.* (2007) Quantitative pH measurements in *Plasmodium falciparum* infected erythrocytes using pHluorin. *Cell. Microbiol.* 9, 1004–1013
- 14 Rohrbach, P. *et al.* (2005) Quantitative calcium measurements in subcellular compartments of *Plasmodium falciparum*-infected erythrocytes. *J. Biol. Chem.* 280, 27960
- 15 Ku, M.J. *et al.* (2011) Quantum dots: a new tool for anti-malarial drug assays. *Malaria J.* 10, 118
- 16 Tokumasu, F. and Dvorak, J. (2003) Development and application of quantum dots for immunocytochemistry of human erythrocytes. *J. Microsc.* 211, 256–261
- 17 Tokumasu, F. *et al.* (2005) Band 3 modifications in *Plasmodium falciparum*-infected AA and CC erythrocytes assayed by autocorrelation analysis using quantum dots. *J. Cell Sci.* 118, 1091
- 18 Hell, S.W. (2003) Toward fluorescence nanoscopy. *Nat. Biotechnol.* 21, 1347–1355
- 19 Schermelleh, L. *et al.* (2008) Subdiffraction multicolor imaging of the nuclear periphery with 3D structured illumination microscopy. *Science* 320, 1332–1336
- 20 Riglar, D.T. *et al.* (2011) Super-resolution dissection of coordinated events during malaria parasite invasion of the human erythrocyte. *Cell Host Microbe* 9, 9–20
- 21 Huang, B. *et al.* (2009) Super resolution fluorescence microscopy. *Annu. Rev. Biochem.* 78, 993
- 22 Mauritz, J. *et al.* (2010) Biophotonic techniques for the study of malaria-infected red blood cells. *Med. Biol. Eng. Comput.* 48, 1055–1063
- 23 van Munster, E.B. and Gadella, T.W.J. (2005) Fluorescence lifetime imaging microscopy (FLIM). In *Microscopy Techniques* (Rietdorf, J., ed.), pp. 1301–1303, Springer
- 24 Esposito, A. *et al.* (2008) FRET imaging of hemoglobin concentration in *Plasmodium falciparum*-infected red cells. *PLoS ONE* 3
- 25 Lawrence, C. and Olson, J. (1986) Birefringent hemozoin identifies malaria. *Am. J. Clin. Pathol.* 86, 360
- 26 Romagosa, C. *et al.* (2004) Polarisation microscopy increases the sensitivity of hemozoin and *Plasmodium* detection in the histological assessment of placental malaria. *Acta Tropica* 90, 277–284
- 27 Mendelow, B.V. *et al.* (1999) Automated malaria detection by depolarization of laser light. *Br. J. Haematol.* 104, 499–503
- 28 Smith, F. (1955) Microscopic interferometry. *Research (Lond.)* 8, 385–395
- 29 Allen, R. *et al.* (1969) The zeiss-Nomarski differential interference equipment for transmitted-light microscopy. *Z. Wiss. Mikrosk. Mikrosk. Technik* 69, 193
- 30 Glushakova, S. *et al.* (2007) Quantification of malaria parasite release from infected erythrocytes: inhibition by protein-free media. *Malaria J.* 6, 61
- 31 Abkarian, M. *et al.* (2011) A novel mechanism for egress of malarial parasites from red blood cells. *Blood* 117, 4118
- 32 Wolter, A. (1932) Über die Schnell diagnose der Malaria mit Hilfe des Dunkelfeldes. *Dermatology* 63, 69–72
- 33 Jamjoom, G.A. (1983) Dark-field microscopy for detection of malaria in unstained blood films. *J. Clin. Microbiol.* 17, 717
- 34 Wilson, B.K. *et al.* (2011) Detection of malarial byproduct hemozoin utilizing its unique scattering properties. *Optics Express* 19, 12190–12196
- 35 Popescu, G. *et al.* (2008) Imaging red blood cell dynamics by quantitative phase microscopy. *Blood Cells Mol. Dis.* 41, 10–16
- 36 Popescu, G. (2011) *Quantitative Phase Imaging of Cells and Tissues*, McGraw-Hill Professional
- 37 Park, Y.K. *et al.* (2006) Diffraction phase and fluorescence microscopy. *Optics Express* 14, 8263–8268
- 38 Popescu, G. *et al.* (2006) Diffraction phase microscopy for quantifying cell structure and dynamics. *Optics Lett.* 31, 775–777
- 39 Park, Y. *et al.* (2010) Measurement of red blood cell mechanics during morphological changes. *Proc. Natl. Acad. Sci. U.S.A.* 107, 6731
- 40 Park, Y.K. *et al.* (2010) Metabolic remodeling of the human red blood cell membrane. *Proc. Natl. Acad. Sci. U.S.A.* 107, 1289
- 41 Park, Y.K. *et al.* (2008) Refractive index maps and membrane dynamics of human red blood cells parasitized by *Plasmodium falciparum*. *Proc. Natl. Acad. Sci. U.S.A.* 105, 13730
- 42 Ding, H. *et al.* (2008) Fourier transform light scattering of inhomogeneous and dynamic structures. *Phys. Rev. Lett.* 101, 238102
- 43 Tycko, D. *et al.* (1985) Flow-cytometric light scattering measurement of red blood cell volume and hemoglobin concentration. *Appl. Optics* 24, 1355–1365
- 44 Tishler, R. and Carlson, F. (1987) Quasi-elastic light scattering studies of membrane motion in single red blood cells. *Biophys. J.* 51, 993–997
- 45 Park, Y. *et al.* (2010) Static and dynamic light scattering of healthy and malaria-parasite invaded red blood cells. *J. Biomed. Optics* 15, 020506
- 46 Choi, W. *et al.* (2007) Tomographic phase microscopy. *Nat. Methods* 4, 717–719
- 47 Chandramohanadas, R. *et al.* (2011) Biophysics of malarial parasite exit from infected erythrocytes. *PLoS ONE* 6, e20869
- 48 Squier, J. *et al.* (1998) Third harmonic generation microscopy. *Optics Express* 3, 315–324
- 49 Béliisle, J.M. *et al.* (2008) Sensitive detection of malaria infection by third harmonic generation imaging. *Biophys. J.* 94, L26–L28
- 50 Bonifacio, A. *et al.* (2008) Spatial distribution of heme species in erythrocytes infected with *Plasmodium falciparum* by use of resonance Raman imaging and multivariate analysis. *Anal. Bioanal. Chem.* 392, 1277–1282
- 51 Wood, B.R. *et al.* (2009) Resonance Raman microscopy in combination with partial dark-field microscopy lights up a new path in malaria diagnostics. *Analyst* 134, 1119–1125
- 52 Ramser, K. *et al.* (2004) Resonance Raman spectroscopy of optically trapped functional erythrocytes. *J. Biomed. Optics* 9, 593
- 53 Heussler, V. and Doerig, C. (2006) *In vivo* imaging enters parasitology. *Trends Parasitol.* 22, 192–195
- 54 Franke-Fayard, B. *et al.* (2006) Real-time *in vivo* imaging of transgenic bioluminescent blood stages of rodent malaria parasites in mice. *Nat. Protoc.* 1, 476–485
- 55 Ploemen, I.H.J. *et al.* (2009) Visualisation and quantitative analysis of the rodent malaria liver stage by real time imaging. *PLoS ONE* 4, e7881
- 56 Thiberge, S. *et al.* (2007) *In vivo* imaging of malaria parasites in the murine liver. *Nat. Protoc.* 2, 1811–1818
- 57 Frevert, U. *et al.* (2005) Intravital observation of *Plasmodium berghei* sporozoite infection of the liver. *PLoS Biol.* 3, e192
- 58 Sturm, A. *et al.* (2006) Manipulation of host hepatocytes by the malaria parasite for delivery into liver sinusoids. *Science* 313, 1287
- 59 Heng, X. *et al.* (2006) Optofluidic microscopy: a method for implementing a high resolution optical microscope on a chip. *Lab Chip* 6, 1274–1276
- 60 Tseng, D. *et al.* (2010) Lensfree microscopy on a cellphone. *Lab Chip* 10, 1787–1792
- 61 Suresh, S. *et al.* (2005) Connections between single-cell biomechanics and human disease states: gastrointestinal cancer and malaria. *Acta Biomater.* 1, 15–30
- 62 Mauritz, J.M.A. *et al.* (2010) Detection of *Plasmodium falciparum*-infected red blood cells by optical stretching. *J. Biomed. Optics* 15, 030517
- 63 Ashkin, A. *et al.* (1986) Observation of a single-beam gradient force optical trap for dielectric particles. *Optics Lett.* 11, 288–290

- 64 Kling, J. (2006) Moving diagnostics from the bench to the bedside. *Nat. Biotechnol.* 24, 891–898
- 65 Zhang, X. *et al.* (2007) Moving cancer diagnostics from bench to bedside. *Trends Biotechnol.* 25, 166–173
- 66 Golenda, C.F. *et al.* (1997) Continuous *in vitro* propagation of the malaria parasite *Plasmodium vivax*. *Proc. Natl. Acad. Sci. U.S.A.* 94, 6786
- 67 Gligorijevic, B. *et al.* (2008) Stage independent chloroquine resistance and chloroquine toxicity revealed via spinning disk confocal microscopy. *Mol. Biochem. Parasitol.* 159, 7–23
- 68 Esposito, A. *et al.* (2008) FRET imaging of hemoglobin concentration in *Plasmodium falciparum*-infected red cells. *PLoS ONE* 3, e3780
- 69 McIntosh, M.T. *et al.* (2007) Traffic to the malaria parasite food vacuole. *J. Biol. Chem.* 282, 11499
- 70 Hay, S.I. *et al.* (2004) The global distribution and population at risk of malaria: past, present, and future. *Lancet Infect. Dis.* 4, 327–336
- 71 WHO (2010) *World Malaria Report 2010*, World Health Organization
- 72 Trampuz, A. *et al.* (2003) Clinical review: severe malaria. *Crit. Care* 7, 315–323
- 73 Greenwood, B.M. *et al.* (2008) Malaria: progress, perils, and prospects for eradication. *J. Clin. Invest.* 118, 1266
- 74 Suwanarusk, R. *et al.* (2004) The deformability of red blood cells parasitized by *Plasmodium falciparum* and *P. vivax*. *J. Infect. Dis.* 189, 190
- 75 Miller, L.H. *et al.* (2002) The pathogenic basis of malaria. *Nature* 415, 673–679